JOURNAL OF CATALYSIS **178,** 34–48 (1998)
ARTICLE NO. CA982102

Effect of Thermal Treatment on the Nickel State and CO Hydrogenation Activity of Titania-Supported Nickel Catalysts

Sui-Wen Ho,[1] Chih-Yang Chu, and Shih-Guan Chen

Department of Chemistry, National Cheng Kung University, Tainan, Taiwan 701, Republic of China

Received June 23, 1997; revised March 6, 1998; accepted April 15, 1998

A series of 6 wt% Ni/TiO_2 catalysts were prepared by pore volume impregnation under various calcination conditions (225–600°C, 1–16 h), and were characterized by XRD, XPS, TG-MS, and chemisorption (H_2 and O_2). The results of XRD, XPS, and TG-MS show the presence of incompletely decomposed nickel nitrates and NiO for catalysts calcined at 225–250°C, and the presence of NiO for catalysts calcined at 300–500°C. $NiTiO_3$ becomes the dominant nickel species in the catalyst calcined at 600°C. Reducibility of nickel to nickel metal depends on the chemical states of nickel in the calcined catalysts. For catalysts calcined below 600°C, where NiO is the main nickel species, 100% reducibility can be obtained at a reduction temperature of 400°C. However, for catalysts calcined at 600°C, where $NiTiO_3$ is the dominant nickel species, complete reduction of nickel species can be achieved at 600°C. Lower turnover frequencies ($TOF(H_2)$) for CO hydrogenation were observed for the catalysts with unreduced nickel phase. When nickel is completely reduced, $TOF(H_2)$ is independent of the chemical states of nickel in the calcined catalysts or reduction temperature. The $TOF(H_2)$'s are an order of magnitude higher than that reported for unsupported nickel indicating the promotion effect of titania on CO hydrogenation even after high reduction temperature. However, an increase in ethene formation rate, methane and C2-C4 percentages, and the olefin to paraffin ratio (C2-C4) was observed, along with a significant decrease in the H/O adsorption ratio as reduction temperature was increased to 600°C for all catalysts. This suggests further interaction of TiO_x moieties with nickel surface in addition to blocking.

INTRODUCTION

Titania-supported nickel catalysts were reported to be more active in CO hydrogenation relative to silica- or alumina-supported catalysts (1–2). In addition, enhanced selectivity toward the higher molecular hydrocarbons which are paraffinic were observed. This was generally related to the strong metal–support interaction which was used by Tauster *et al*. to explain the suppression of H_2 and CO adsorption for metals supported on titania when reduced at 773 K instead of 473 K (3). However, the advantages of titania relative to silica for CO hydrogenation observed at a 723 K reduction were no longer exist after reduction at 923 K (4). A decreasing trend of CO hydrogenation activity for Ni/TiO_2 catalyst with increasing reduction temperature were also reported (5). Therefore, the promoting effect of titania may not require the reduction at high temperature, which bring the titania-supported metal catalysts into the SMSI-state. On the other hand, Burch *et al*. reported the enhanced C2+ selectivity with increasing reduction temperature (4), while Turlier *et al*. showed the invariant C2+ selectivity (5). Recently, the dependence of C2+ formation on the nickel loading and reduction temperature was reported for Ni/TiO_2 catalysts (6). However, the relationship between adsorptive and catalytic properties as a function of reduction temperature has not been systematically examined.

A number of studies have indicated that the occurrence of the SMSI state is dependent on the preparation method (7, 8). de Bokx *et al*. found that a solid state reaction proceeds between NiO and TiO_2 during calcination at temperature higher than 573 K, and the interdiffusion might lead to the formation of $NiTiO_3$ which displayed the characteristics of the SMSI after reduction (9). Their observations suggest that the degree of $NiO{-}TiO_2$ interaction in a Ni/TiO_2 catalyst may predetermine the extent of suppression of hydrogen chemisorption and the extent of reduction of nickel phase. Hence, it is worthwhile investigating the relationships among the extent of $NiO{-}TiO_2$ interaction, the adsorptive properties and the catalytic activity and selectivity.

In this study, we systematically investigated the dependence of the adsorptive and catalytic properties of nickel metal on the nickel precursor in the calcined Ni/TiO_2 catalysts and on the reduction temperature (250–600°C). The effect of calcination temperature on the nickel state and their reduction behavior and the effect of reduction temperature on the adsorptive and catalytic properties were studied. The relationship between of adsorptive and catalytic properties was examined.

[1] To whom correspondence should be addressed. E-mail: rayho@ mail.ncku.edu.tw.

0021-9517/98 $25.00

EXPERIMENTAL

Catalyst Preparation

The TiO_2 support (Degussa P-25, BET surface area 53 m^2/g, pore volume 0.4 mL/g) was wetted with ethanol, dried at 100°C for 16 h, and calcined at 400°C for 16 h and 500°C 1 h in air. All samples were prepared by pore volume impregnation. The 6 wt% Ni/TiO_2 catalysts were prepared by impregnation of the pretreated titania with nickel nitrate solution (Alfa). The impregnated powders were dried at 100°C for 16 h and then calcined at various temperatures (225–600°C) for 1 or 16 h in air. The catalysts were designated as *X-Y*, where *X* stands for calcination temperature (°C), and *Y* for calcination time (h). For instance, 400-16 represents a 6 wt% Ni/TiO_2 catalyst calcined at 400°C for 16 h.

Samples were reduced under H_2 flow (50 mL/min, 99.9999% Scott) at various conditions: (1) 250°C for 8 h; (2) 400°C for 8 h; (3) 500°C 1 h; (4) 600°C 1 h before chemisorption and activity measurements. The heating rate is 10°C/min.

X-Ray Diffraction

X-ray powder diffraction patterns were obtained from Shimadz XD-D1 diffractometer equipped with a high temperature cell. Powdered sample were packed into a $2 \times 0.5 \times 0.5$ cm^3 hollowed ceramic plate. The cell was evacuated and purged with H_2 flow (100 mL/min) for 2 h before reduction treatment. After reduction treatment, the cell was cooled to room temperature under H_2 flow for XRD measurement. The ASTM powder diffraction file was used to identify the phase presented. The crystallite sizes were calculated from line broadening using the Scherrer equation (10). Instrumental broadening was corrected from a reference NiO sample (Alfa) calcined at 800°C for 48 h.

X-Ray Photoelectron Spectroscopy

X-ray photoelectron spectra were recorded using a VG ESCA 210 electron spectrometer equipped with an Al anode (1486.6 eV) operated at 12 kV and 18 mA. The catalysts were run as powders dusted on sticky tape. The $Ti2p_{3/2}$ line (458.7 eV) was used as the binding energy reference for the catalysts. The binding energies of standard compounds were referenced to the C 1s line (284.6 eV).

Temperature-Programmed Reduction

Temperature programmed reduction was performed on a Cahn TG-121 thermogravimetric analyzer and a VG Sensorlab 300D mass spectrometer. In general, sample of 0.1 g were used. Reduction was carried out under H_2 flow (50 mL/min) with a heating rate of 10°C/min to 600°C.

Chemisorption

Hydrogen and oxygen chemisorption was performed in a conventional volumetric system evacuated by mechanical and turbo pumps. The base pressure of the system was ca 5×10^{-6} Torr. A MKS-390 Baratron Pressure Transducer was used for pressure measurements over a range of 0 to 300 Torr. Following reduction treatments, the sample was evacuated for 30 min at reduction temperature and adsorption isotherm was taken at room temperature. Because of the high heat of oxygen adsorption on nickel, small aliquots of oxygen were admitted in a slow and stepwise manner (11). The total gas uptake was determined by extrapolating the straight-line portion of the adsorption isotherm to zero pressure. For activated measurement, a second isotherm was taken by raising the temperature to 200°C for 5 min, and then cooled to room temperature for each point. The percentage dispersion of nickel was calculated assuming the $H_{(ad)}/Ni_{(s)} = 1$ and $O_{(ad)}/Ni_{(s)} = 1$ (11, 12). The percentage of reduction of nickel phase to nickel metal was calculated from the amount of oxygen consumed during reoxidation of nickel metal to NiO at 400°C. The formation of NiO after reoxidation of nickel metal was confirmed with XRD. Corrections were made to both the oxygen chemisorption and reoxidation based on the blank measurements on titania support. The relative standard deviations of the measurements for O_2 and H_2 chemisorption were generally below 10 and 15%, respectively.

CO Hydrogenation

Activity measurements were carried out in a flow microreactor consisting of Pyrex glass reactor (1/4 in), stainless steel feed lines, temperature programmer (Watlow), and flow controller (Unit). Samples of 30 mg were reduced at various temperatures (250–600°C). After reduction, samples were allowed to cool to and then maintained at reaction temperature of 200°C. A premixed $CO/H_2/He$ (3/9/88, 99.999%, Air Products) feed gas was introduced at a flow rate of 50 mL/min. The products were analyzed by gas chromatography using OV-101 and VZ-10 columns. Under this reaction condition, the conversions of CO to hydrocarbons were below 2% for all activity measurements. The relative standard deviations of activity measurements were generally below 10%.

RESULTS

X-Ray Diffraction

The X-ray diffraction patterns of 6 wt% Ni/TiO_2 calcined at various temperature are shown in Fig. 1. In addition to the diffraction peaks of anatase and rutile, diffraction peaks characteristic of NiO appeared when sample was calcined at 225°C. As the calcination temperature increased, the

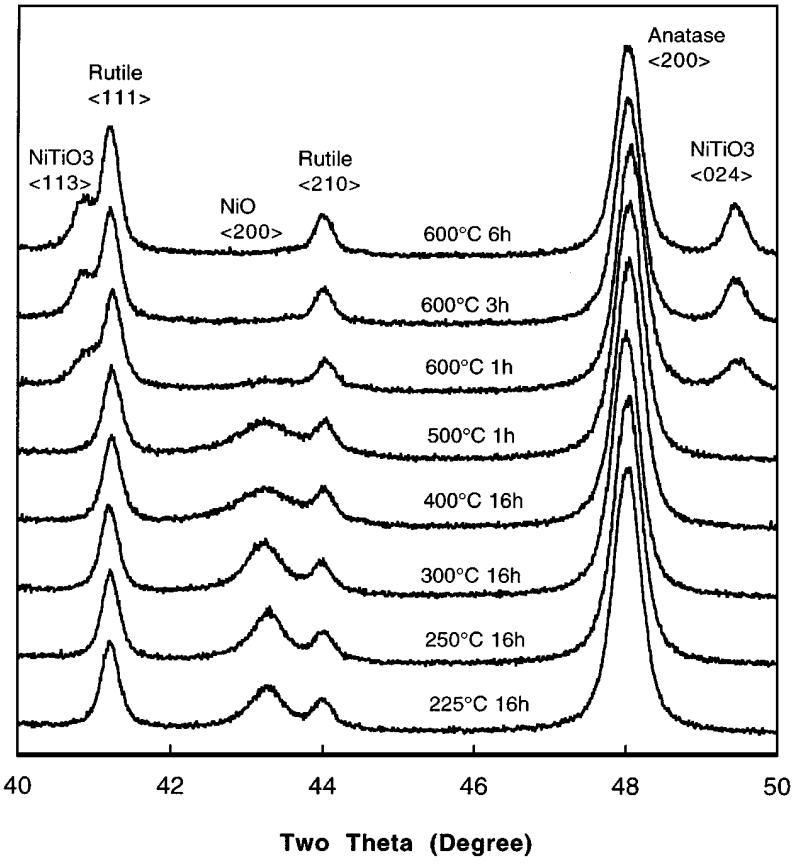

FIG. 1. X-ray diffraction patterns of the calcined 6 wt% Ni/TiO_2 catalysts.

NiO ⟨200⟩ peak became broader and disappeared after the sample was calcined at 600°C for 3 h. New diffraction peaks characteristic of $NiTiO_3$ emerged when the sample was calcined at 600°C and became more intense and narrower as the calcination time increased.

The amounts of NiO and $NiTiO_3$ were estimated by comparing the NiO ⟨200⟩/Rutile ⟨111⟩ or $NiTiO_3$ ⟨104⟩/Rutile ⟨110⟩ intensity ratios with that of the physical mixtures of NiO or $NiTiO_3$ and TiO_2, respectively. The results are given in Table 1. The detected percentage of NiO by XRD increases from 41 to 57% as the calcination temperature increases from 225 to 300°C, then it decreases to 47% as the temperature further increases to 500°C. For the sample calcined at 600°C for 1 h, 62% of the Ni species is present as $NiTiO_3$. The percentage of $NiTiO_3$ increases to 85% when the sample was further calcined for 6 h at 600°C. The crystallite size estimated from the full width at half maximum of the NiO ⟨200⟩ and $NiTiO_3$ ⟨024⟩ is also given in Table 1. The crystallite size of NiO remains relatively unchanged at 17–18 nm when calcined under 300°C, but it decreases to 10–12 nm as the temperature increases to 400 and 500°C. On the other hand, the crystallite size of $NiTiO_3$ increases from 26 to 37 nm as the calcination time increases from 1 to 6 h at 600°C.

The crystallite size of nickel metal for some reduced samples based on the line width of Ni ⟨111⟩ peak are given in Table 2. For 250-16, the Ni crystallite size increases from 7 to 10 nm as the reduction temperature increases from 250

TABLE 1

The Percentage and Crystallite Size of Ni Phases Estimated from X-Ray Diffraction Patterns for 6 wt% Ni/TiO_2 Catalysts after Various Calcination Treatments

	Percentage of Ni phase[b]		Crystallite size (nm)[b]	
Catalyst[a]	NiO	$NiTiO_3$	NiO	$NiTiO_3$
225-16	41		17	
250-16	50		18	
300-16	57		18	
400-16	49		10	
500-1	47		12	
600-1		62		26
600-3		80		34
600-6		85		37

[a] Catalysts were named by the calcination temperature (°C) and duration (h).

[b] The relative standard deviations for the measurements of percentage and crystallite size of nickel phases is less than 10 and 5%, respectively.

TABLE 2

Particle Size of Nickel Metal Estimated from X-Ray Diffraction, Hydrogen and Oxygen Chemisorption for 6 wt% Ni/TiO_2 Reduced at Various Temperatures

Catalyst/ technique	Particle size of nickel metal (nm)			
	250°C	400°C	500°C	600°C
250-16				
XRD[a]	7		8	10
O_2[b]	5		8	14
H_2[b]	25		50	250
400-16				
XRD		8	9	11
O_2		6	6	11
H_2		25	33	200

[a] Crystallite size calculated from line broadening of Ni ⟨111⟩ line using the Scherrer equation (10).

[b] Particle size of Ni estimated from oxygen and hydrogen chemisorption. Spherical particles were assumed, and the equation was d_s (nm) = 101/%D adopted from Ref. (12).

to 600°C. An increase of Ni crystallite size from 8 to 11 nm as reduction temperature increases from 400 to 600°C was also obtained for 400-16.

X-Ray Photoelectron Spectroscopy

The XPS $Ni2p_{3/2}$ spectra for NiO and $NiTiO_3$ standard compounds and the representative 6 wt% Ni/TiO_2 catalysts are shown in Fig. 2. The $Ni2p_{3/2}$ binding energy and peak width for standard compounds and the 6 wt% Ni/TiO_2 catalysts are given in Table 3. The $Ni2p_{3/2}$ spectra for NiO exhibits a characteristic doublet structure (855.4 and 853.8 eV) with a peak width (FWHM) of 4.7 eV and a satellite located at 860.7 eV (13). The higher binding energy peak of the NiO doublet was attributed to Ni^{3+} species associated with the

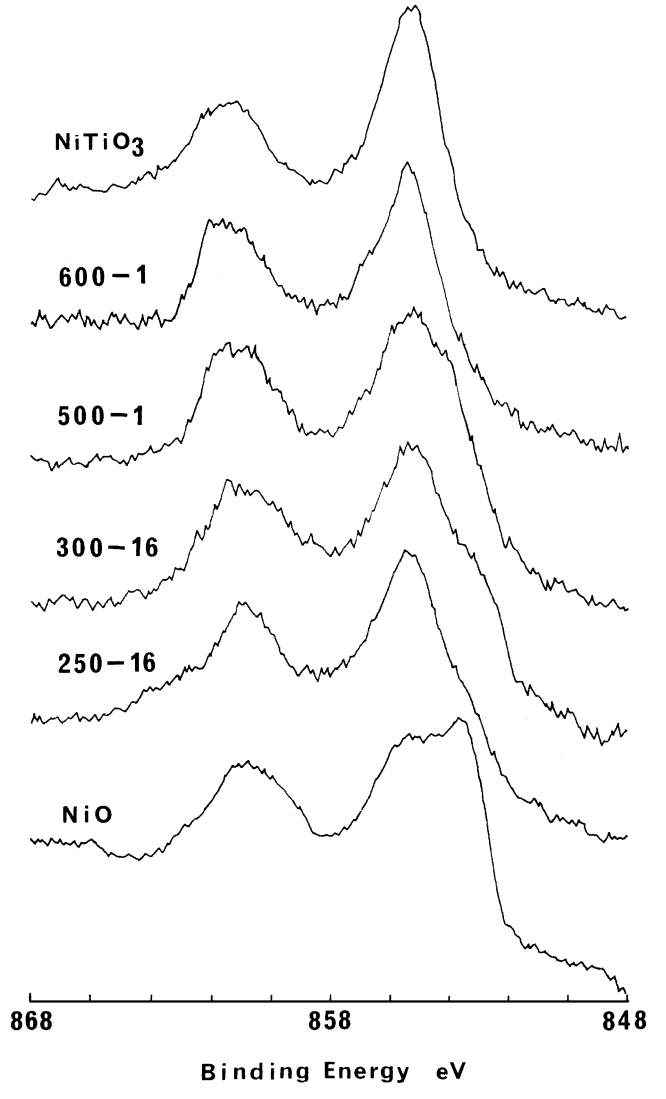

FIG. 2. X-ray photoelectron $Ni2p_{3/2}$ spectra for the representative 6 wt% Ni/TiO_2 catalysts.

TABLE 3

Binding Energy and Peak Width of $Ni2p_{3/2}$, and ΔE between $Ni2p_{3/2}$ Main Peak and Shake-Up Satellite for 6 wt% Ni/TiO_2 Calcined at Various Conditions

Sample	$Ni2p_{3/2}$ B.E. (eV)	FWHM (eV)	ΔE[a] (eV)
NiO	855.4, 853.8	4.7	5.3
$NiTiO_3$	855.5	2.7	6.2
250-16	855.7	3.8	5.5
300-16	855.7	4.5	5.5
400-16	855.6	4.1	5.8
500-1	855.7	4.1	5.8
600-1	856.0	2.7	5.8
600-3	856.1	3.2	6.0
600-6	855.9	2.9	6.1

[a] Energy difference between $Ni2p_{3/2}$ main peak and shake-up satellite. For NiO, the higher binding energy peak of the doublet was referred. The standard deviation for measurement of binding energy is ±0.2 eV.

nonstoichiometry of NiO sample (14, 15). Whereas that of $NiTiO_3$ shows a single line at 855.5 eV with a narrower width of 2.7 eV and a satellite located ca 6.2 eV higher than the main peak. For 250-16 and 300-16, the $Ni2p_{3/2}$ exhibit a main peak at 855.7 eV which is consistent with the reported $Ni2p_{3/2}$ binding energy for titania-supported nickel (16) and is 1.9 eV higher than the main peak of NiO. In addition, a shoulder at 853.8 eV is observed which is the position of the main peak of NiO. This indicates the presence of discrete NiO, in addition to the finely dispersed nickel phase in these samples. For 500-1 and 400-16 one broad peak is obtained indicating that more than one nickel phase is present. For 600-1, 600-3, and 600-6, the $Ni2p_{3/2}$ spectra resemble that of $NiTiO_3$. In general, the $Ni2p_{3/2}$ binding energy varies insignificantly with the increasing calcination temperature, but a decrease in peak width and an increase in the binding energy difference (ΔE) between the main peak and

the shake-up satellite are observed as the calcination temperature increases. This indicates a change in the chemical state of Ni from NiO to $NiTiO_3$, in line with the results of XRD.

Temperature-Programmed Reduction

The rate of weight loss of 6 wt% Ni/TiO_2 catalysts during temperature-programmed reduction under H_2 flow is shown in Fig. 3. In general, the temperature of the reduction band increases as the calcination temperature increases. For 250-16 a broad multiplet band was observed at 260°C. The weight loss band located at 206°C was accompanied with the evolution of NO, CO, and CO_2, in addition to H_2O in the gas stream. This indicates the incompleteness of decomposition of nickel nitrates and the presence of adsorbed organic species in 250-16. For 300-16 two reduction bands located at 270 and 374°C were observed. For 400-16 and 500-1 a band located at 385–393°C with a shoulder at 270°C was observed. The bands located at 270°C, which is comparable to the reported reduction temperature (285–305°C) for unsupported NiO (9, 17–20), therefore, is assigned to bulk NiO without any interaction with the titania surface. The higher temperature bands (374–393°C) are tentatively assigned to the NiO with significant interaction with the titania surface, or the $NiO–TiO_2$ interaction species. As the calcination temperature increased to 600°C, a broader band appeared, and the band temperature increased from 460 to 510°C with increasing the calcination time from 1 to 6 h. These bands are assigned to the bulk $NiTiO_3$ (9, 20–22).

Chemisorption

The percentage of reduction of nickel phase to nickel metal for the 6 wt% Ni/TiO_2 catalysts is given in Table 4. As it can be seen, except the catalysts reduced at 250°C and 600-1, 600-3, and 600-6 reduced at temperatures $\leq$500°C, nickel phase were quantitatively reduced to nickel metal. These results are consistent with that of TPR.

The amount of H_2 and O_2 adsorption for the 6 wt% catalysts reduced at various temperature (250–600°C) are given in Table 5. The amount of H_2 adsorption (1.5–17.7 μmol/g-cat) are found to be all lower than the amount of O_2 adsorption (28.8–87.9 μmol/g-cat). The percentage dispersion of nickel metal is calculated assuming H/Ni or O/Ni ration of 1 (11, 12). The variation of percentage dispersion obtained from hydrogen chemisorption (%D(H_2)) and oxygen

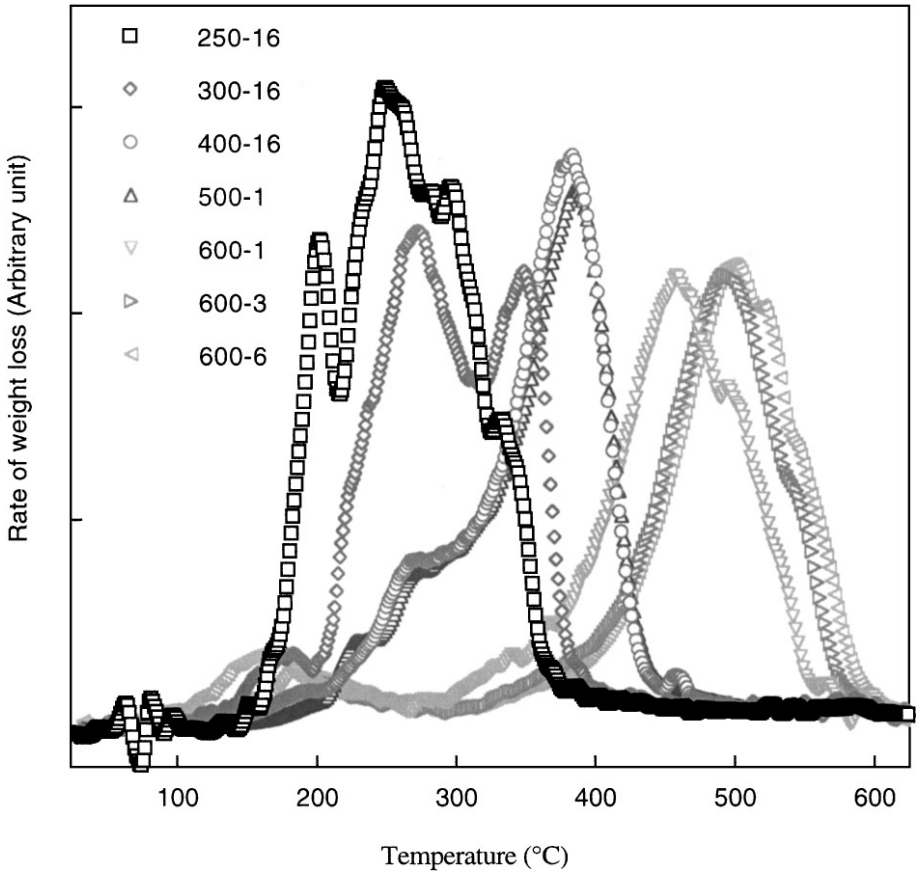

FIG. 3. Temperature-programmed reduction curves of the 6 wt% Ni/TiO_2 catalysts.

TABLE 4

Percentage of Nickel Reduction to Nickel Metal Determined from Reoxidation after Reduction at Various Temperatures

Catalysts	Percentage of nickel reduction (%)			
	250°C	400°C	500°C	600°C
250-16	79	97 (95)[a]	98 (95)	101 (94)
300-16	64	99 (96)	101 (98)	105 (99)
400-16	30	100 (97)	101 (98)	105 (99)
500-1	34	99 (96)	101 (98)	103 (97)
600-1			96 (93)	105 (98)
600-3			90 (87)	103 (97)
600-6		36 (33)	89 (86)	104 (97)

[a] Number in parentheses is the percentage of nickel reduction after correction for the oxygen uptake of titania support during reoxidation at 400°C after reduction at various temperatures. The oxygen amounts are 0, 14.4, 15.6, and 33.7 μmol/g-TiO_2 for reduction temperatures of 250, 400, 500, and 600°C, respectively. The relative standard deviation is below 10%.

chemisorption (%$D(O_2)$) as a function of the calcination temperature for 6 wt% catalysts reduced at various temperatures are shown Figs. 4 and 5, respectively. In general, a decrease in %$D(H_2)$ and %$D(O_2)$ with increasing reduction temperature was observed for each catalyst. Under same reduction temperature ($\leq$500°C), higher %$D(H_2)$ and %$D(O_2)$ were obtained for catalysts calcined at 400 or 500°C. However, %$D(H_2)$ and %$D(O_2)$ remained essentially unchanged as functions of calcination temperature when the catalysts were reduced at 600°C. The %$D(H_2)$'s of the catalysts are quite low and ranged from 0.4 to 5.3%. The

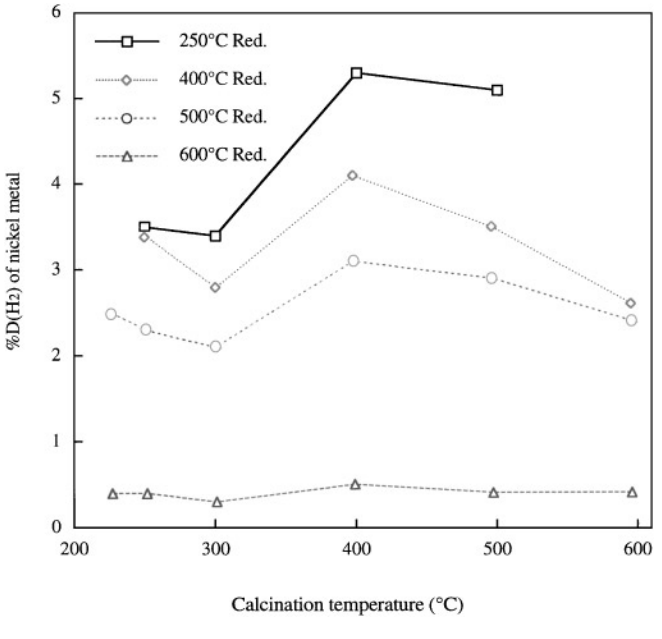

FIG. 4. Variation of percentage of $D(H_2)$ as a function of calcination temperature for 6 wt% Ni/TiO_2 catalysts reduced at various temperatures.

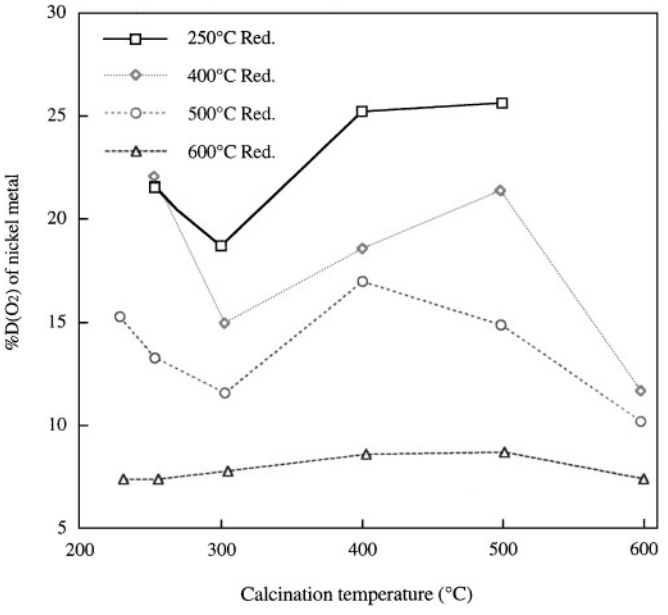

FIG. 5. Variation of percentage of $D(O_2)$ as a function of calcination temperature for 6 wt% Ni/TiO_2 catalysts reduced at various temperatures.

amount of hydrogen adsorbed at room temperature (RT) increased to ca 1.6 times for most catalysts when the adsorption temperature was raised to 200°C and then cooled to RT. This may indicate that the hydrogen adsorption on Ni/TiO_2 is an activated process, which has been reported (20). Even it is so, the %$D(H_2)$ obtained from activated adsorption is also much lower then the corresponding value obtained from oxygen chemisorption. Besides, the activated process may be due to the hydrogen spillover (23). Hence, the %$D(H_2)$ obtained from H_2 adsorption at room temperature was adopted for the calculation of turnover frequency for CO hydrogenation.

CO Hydrogenation

The activity of CO hydrogenation for 600-6 reduced at various temperature as a function of time on stream is shown Fig. 6. A steady state was reached after ca 5 h on stream for all reduction temperature. However, unlike the observed decay of activity (to ca 60% of initial activity) for reduction temperatures $\leq$500°C, an induction period of ca 1 h was observed for 600-6 reduced at 600°C. This is typical of all catalysts reduced at 600°C, indicating that this behavior is dependent of the reduction temperature but not of the precursor of nickel metal.

The activity and CO conversion of steady state for CO hydrogenation for catalysts reduced at various temperature are given in Table 6. The specific activity (μmol/g-Ni/s) of steady state versus the calcination temperature for various reduction temperature is shown in Fig. 7. The specific activity was found to vary insignificantly with increasing the calcination temperature for each reduction temperature with

TABLE 5

The Amount (μmol/g-cat) of Hydrogen and Oxygen Adsorption and Percentage Dispersion of Nickel for 6 wt% Ni/TiO_2 Catalysts Reduced at Various Temperatures

	Amount of adsorption (μmol/g-cat)						
Red. temp.	250-16	300-16	400-16	500-1	600-1	600-3	600-6
250°C							
H_2 (RT)	13	10	7.7	8.1			
	(3.5%)[a]	(3.4%)	(5.3%)	(5.1%)			
H_2 (200°C)	49.7	40.3	19.4	17.6			
O_2 (RT)[b]	81	57	36	41			
	(21.5%)	(18.7%)	(25.2%)	(25.6%)			
400°C							
H_2 (RT)	16	13	18	17			4.1
	(3.4%)	(2.8%)	(3.7%)	(3.5%)			(2.6%)
H_2 (200°C)	26.3	21.7	28.9	27.1			7.3
O_2 (RT)	104.5	71.0	87.9	101.2			18.2
	(22%)	(15%)	(19%)	(21%)			(12%)
500°C							
H_2 (RT)	11	9.7	15	14	10	10	9.3
	(2.3%)	(2.1%)	(3.1%)	(2.9%)	(2.4%)	(2.4%)	(2.3%)
H_2 (200°C)	19.3	16.3	23.4	22.4	17.1	16.6	15.8
O_2 (RT)	63	55	80	71	45	38	31
	(13.2%)	(11.5%)	(16.9%)	(14.8%)	(10.1%)	(9.2%)	(7.5%)
600°C							
H_2 (RT)	2.1	1.6	2.5	1.9	2.0	1.6	1.5
	(0.4%)	(0.3%)	(0.5%)	(0.4%)	(0.4%)	(0.3%)	(0.3%)
H_2 (200°C)	3.7	3.4	4.2	3.2	3.1	2.7	2.3
O_2 (RT)	35	37	41	42	35	33	29
	(7.4%)	(7.8%)	(8.6%)	(8.7%)	(7.4%)	(7.0%)	(6.1%)

[a] Numbers in parentheses are the percentage dispersion of nickel metal. The adsorption stoichiometries, $H_{(ad)}/Ni_{(s)} = 1$ and $O_{(ad)})/Ni_{(s)} = 1$, are assumed (11, 12). The relative standard deviations of measurements for O_2 and H_2 chemisorption are generally below 10 and 15%.

[b] Values corrected for the oxygen adsorption of titania. The amounts of oxygen adsorption for titania are 0, 8.3, 10.8, 18.8 μmol/g-TiO_2 after reduction at 250, 400, 500, and 600°C, respectively.

some exceptions. Another feature in Fig. 7 is the specific activity for the catalysts reduced at 600°C is significantly lower than those for catalysts reduced below 600°C.

The turnover frequency (TOF) calculated based on the nickel dispersion obtained from hydrogen chemisorption versus the calcination temperature is shown in Fig. 8. Lower activity was generally found for those catalysts with low percentages of reduction, e.g., 400-16 and 500-16 reduced at 250°C, and 600-1, 600-3, and 600-6 reduced below 600°C. This suggests the detrimental effect of the unreduced nickel phase. Considering only the catalysts with a quantitative reduction of the nickel phase, the TOF(H_2)'s for catalysts reduced below and at 500°C remains essentially unchanged and averages $(9.4 \pm 0.9) \times 10^{-3}$ s^{-1}, while the TOF(H_2) averages $(11.2 \pm 0.4) \times 10^{-3}$ s^{-1} for catalysts reduced at 600°C, which is ca 20% higher than that for catalysts reduced below 600°C.

The TOF(H_2)'s for methane formation as a function of calcination temperature at various reduction temperatures are shown in Fig. 9. The TOF(H_2) also varies insignificantly and averages $(1.4 \pm 0.3) \times 10^{-3}$ s^{-1} for catalysts reduced below and at 500°C. Higher TOF(H_2)'s are obtained for catalysts reduced at 600°C, and the average value increases to $(3.1 \pm 0.6) \times 10^{-3}$ s^{-1}, which is about twice that for catalysts reduced below 600°C. The selectivities for the catalysts reduced at 500 and 600°C are given in Tables 7 and 8. The selectivities of other reduction temperatures are similar to that of 500°C, and therefore are omitted. The percentages of C1, C2-C4, and C5+ formation are plotted against the calcination temperature and are shown in Fig. 10. It can be seen that both percentages of C1 and C2-C4 fractions increase at the compensation of C5+ fraction with increasing the reduction temperature from 500 to 600°C. Particularly, a decrease in higher hydrocarbon formation is accompanied by favorable olefin formation. The ethene/ethane ratio as a function of the calcination temperature for catalysts reduced at various temperatures is shown in Fig. 11. Significantly higher ratios are obtained for catalysts reduced at 600°C (3.8 ± 0.2) than that for catalysts reduced below 600°C (0.3 ± 0.1). Similar results

TABLE 6

Activity of CO Hydrogenation for 6 wt% Ni/TiO_2 Catalysts Reduced at Various Temperatures

	Rate of CO hydrogenation (μmol/g-Ni/s)						
Red. temp.	250-16	300-16	400-16	500-1	600-1	600-3	600-6
250°C	5.6 (1.3%)[a] [9.3][b]	5.6 (1.0%) [9.6]	2.2 (0.19%) [2.5]	2.5 (0.24%) [2.9]			
400°C	5.9 (1.6%) [10.3]	4.8 (1.3%) [10]	5.3 (1.5%) [8.4]	6.1 (1.7%) [9.9]			3.2 (0.86%) [3.6]
500°C	3.8 (1.0%) [9.7]	3.7 (1.0%) [10.4]	3.8 (1.1%) [7.3]	4.4 (1.2%) [8.9]	3.3 (0.88%) [8]	2.5 (0.63%) [6.1]	2.3 (0.57%) [5.8]
600°C	0.8 (0.22%) [11.2]	0.8 (0.23%) [11.9]	0.8 (0.20%) [10.4]	0.8 (0.22%) [11.9]	0.6 (0.20%) [11.2]	0.6 (0.17%) [10.9]	0.6 (0.17%) [11.2]

[a] Percentage of CO converted to hydrocarbons.

[b] Turnover frequency ($10^{-3}\,s^{-1}$), TOF(H_2), calculated by using nickel dispersion obtained from hydrogen chemisorption at room temperature.

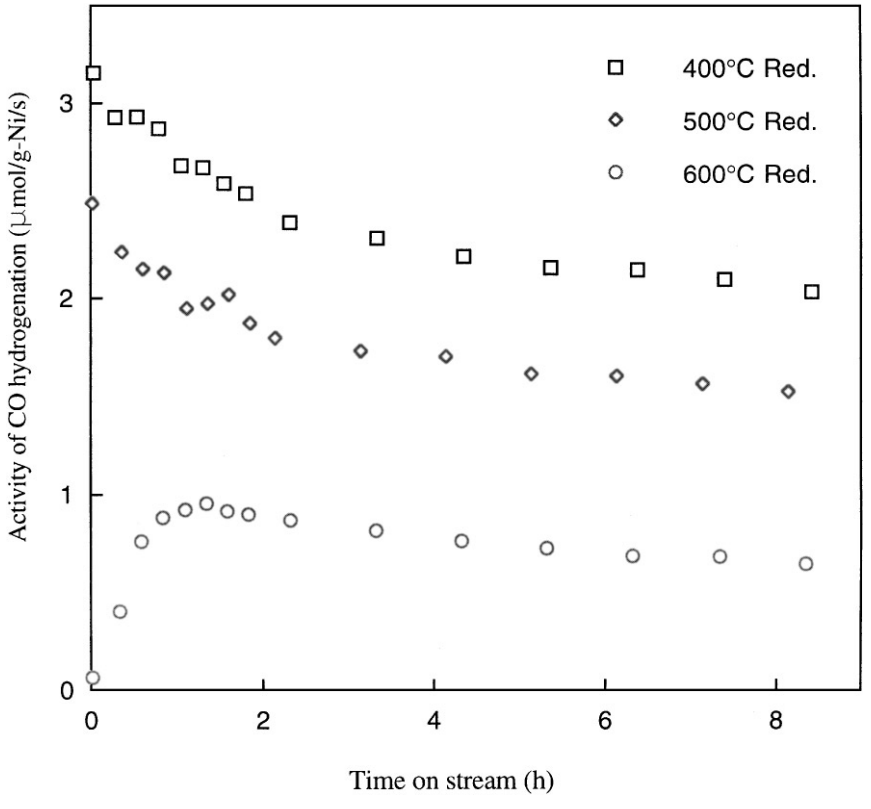

FIG. 6. Variation of CO hydrogenation rate as a function of time on stream for 600-6 catalyst reduced at 400–600°C. The reaction temperature is 200°C.

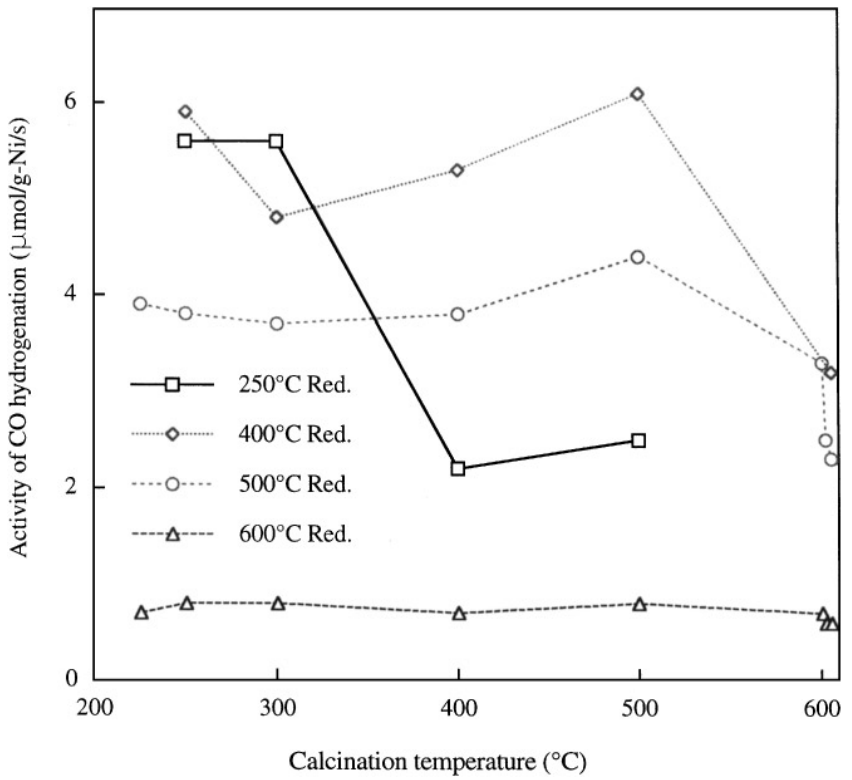

FIG. 7. Steady-state activity for CO conversion to hydrocarbons versus calcination temperature for 6 wt% Ni/TiO_2 catalysts reduced at various temperatures. The reaction temperature is 200°C.

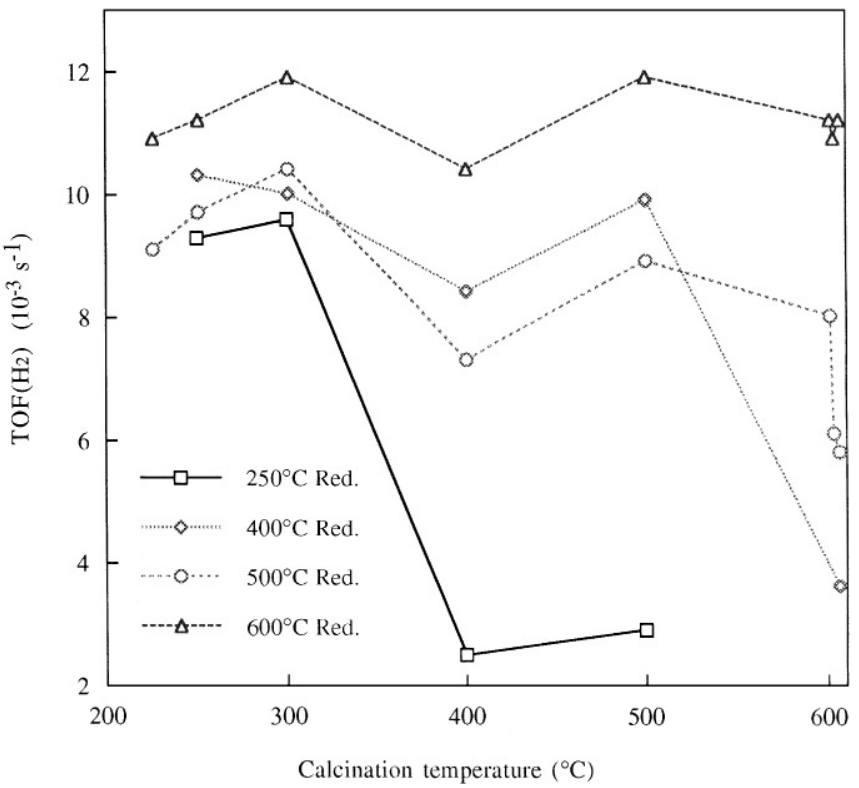

FIG. 8. Variation of the turnover frequency, $TOF(H_2)$ for CO conversion to hydrocarbons, as a function of calcination temperature for 6 wt% Ni/TiO_2 catalysts reduced at various temperatures.

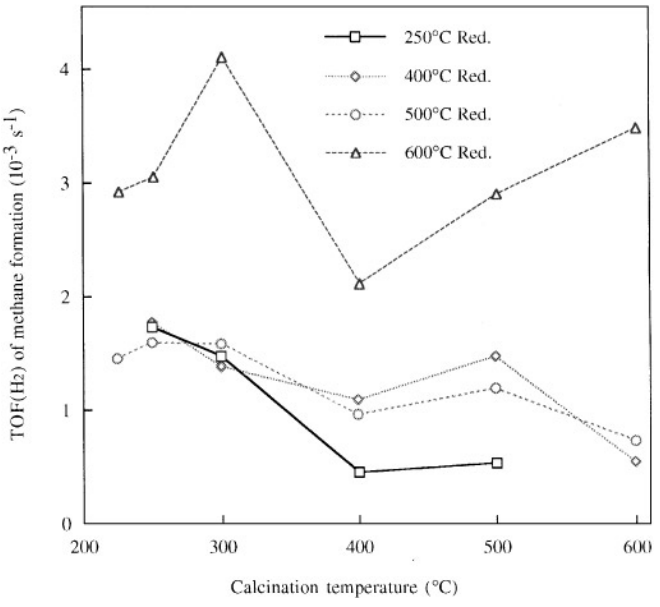

FIG. 9. Variation of the turnover frequency, TOF(H_2) for methane formation, as a function of calcination temperature for 6 wt% Ni/TiO_2 catalysts reduced at various temperatures.

TABLE 8

Olefin/Paraffin Ratio of C2 to C4 Fraction for Catalysts Reduced at Various Temperatures

	Olefin to paraffin ratio				
Red. temp.	250-16	300-16	400-16	500-1	600-6
250°C Red.					
C_2H_4/C_2H_6	0.2	0.2	0.6	0.4	
C_3H_6/C_3H_8	3.1	3.5	5.1	4.1	
C_4H_8/C_4H_{10}	3.9	3.8	5.1	3.3	
400°C Red.					
C_2H_4/C_2H_6	0.2	0.3	0.3	0.3	1.2
C_3H_6/C_3H_8	2.0	3.0	3.0	2.8	5.6
C_4H_8/C_4H_{10}	3.1	3.2	3.0	3.1	4.1
500°C Red.					
C_2H_4/C_2H_6	0.4	0.4	0.4	0.4	0.9
C_3H_6/C_3H_8	3.6	3.5	3.2	3.6	4.9
C_4H_8/C_4H_{10}	3.8	3.6	3.5	3.5	4.4
600°C Red.					
C_2H_4/C_2H_6	3.8	3.5	4.0	3.9	3.7
C_3H_6/C_3H_8	13.7	13.4	14.9	15.0	12.4
C_4H_8/C_4H_{10}	10.4	9.7	10.7	10.7	8.6

are obtained for the propene/propane ratio (3.4 ± 0.8 for catalysts reduced below 500°C, 14 ± 1 for catalysts reduced at 600°C) and the butene/butane ratio (3.6 ± 0.6 for catalysts reduced below 500°C, 10.0 ± 0.9 for catalysts reduced at 600°C).

DISCUSSION

Chemical State of Nickel

XRD indicates that ca 40% of Ni is present as NiO with an average crystallite size of 17 nm for catalyst calcined at 225°C. Both the amount and crystallite size of NiO increase slightly with increasing the calcination temperature to 300°C; then they decrease as the temperature is further raised to 400 or 500°C. The effect is more dramatic for the NiO crystallite size as the temperature is increased from 300 to 400°C. Both XRD and XPS show a major change of Ni phase from mainly NiO to $NiTiO_3$ when the calcination temperature was increased from 500 to 600°C. Rao *et al*. also reported $NiTiO_3$ formation when calcined above 500°C (19), while de Bokx *et al*. reported a formation temperature of 750°C (9). The variation of the nickel state is also accompanied with a color change from gray (≤300°C) to light yellow (400 and 500°C), then bright yellow (600°C). Based on the results of XRD and XPS, further information about the Ni state can be revealed from TPR. For catalysts calcined at 300°C, TPR indicates that ca two-thirds of the Ni is present as discrete NiO (270°C band) and the rest, possibly, as NiO–TiO_2 interaction species (374°C band). The percentage of *discrete* NiO further decreases to less than 10% for catalysts calcined at 400 or 500°C; the rest may be present as NiO which is strongly interacted with the TiO_2 surface, as inferred from the higher reduction temperature (385–393°C bands). For catalysts calcined at 600°C, the tailing toward low temperature side, indicating the existence of some NiO strongly interacted with TiO_2, and the amount decreases with increasing reduction time. In addition, the reduction temperature of $NiTiO_3$ increases with increasing calcination time. The observed increase in the reduction temperature of the nickel phase with increasing the calcination temperature or time indicates the temperature dependence of the interaction between NiO and TiO_2. This is attributed to the temperature dependence of the

TABLE 7

Selectivities for Catalysts Reduced at 500 and 600°C

	%CH_4		%C_2H_4		%C2-C4		%C5+	
Catalysts	500°C[a]	600°C	500°C	600°C	500°C	600°C	500°C	600°C
225-16	16	29	2.2	22	32	67	52	4.7
250-16	17	26	2.6	19	33	60	51	14
300-16	15	26	2.2	19	31	63	54	11
400-16	13	26	1.4	22	30	69	57	5.8
500-1	13	25	1.4	21	29	65	57	11
600-1	20	33	1.9	25	39	58	41	8.5
600-3	13	30	1.9	21	26	65	61	5.0
600-6	8.8	26	1.5	17	19	51	72	23
Average[b]	15	28	2.0	21	30	62	55	10

[a] Reduction temperature.
[b] Averaged percentage.

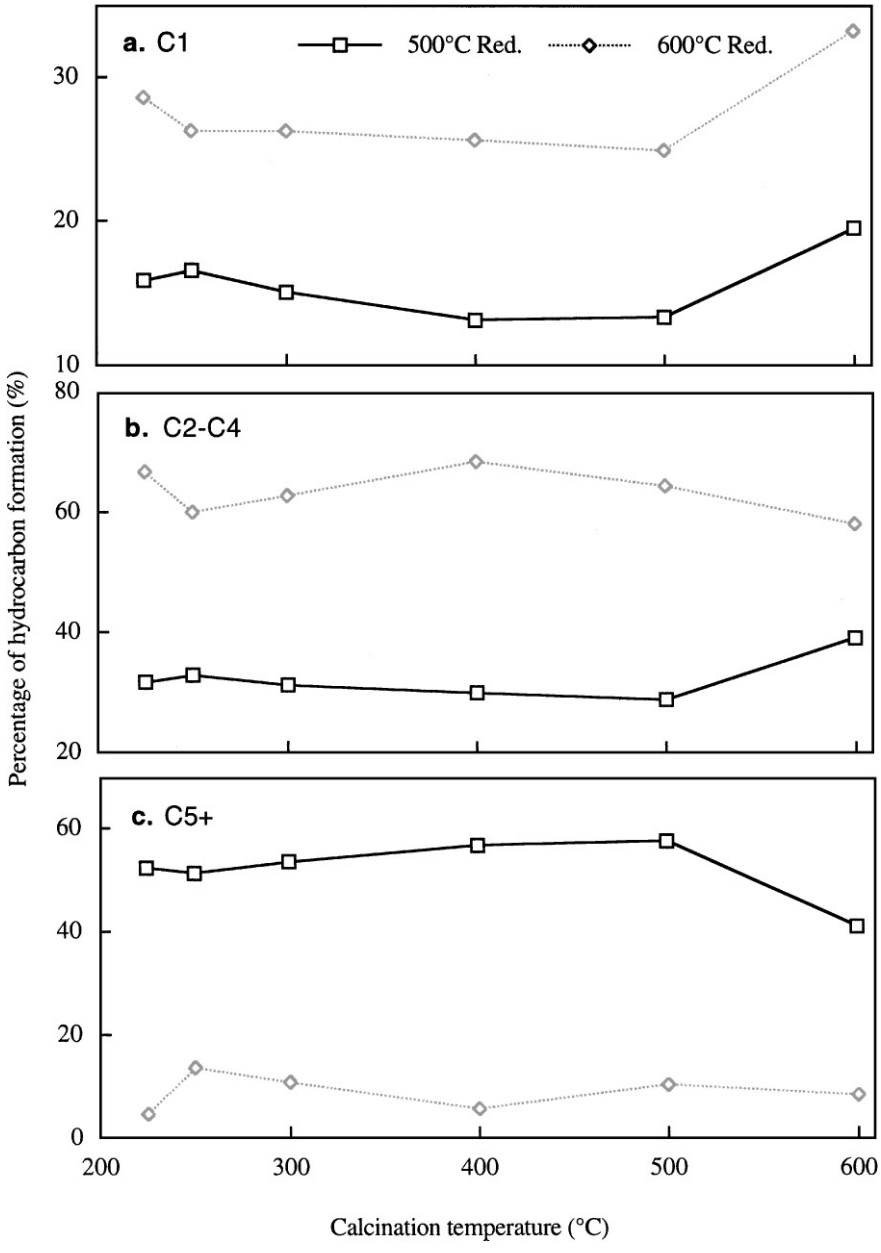

FIG. 10. Variation of percentage of hydrocarbon formation as a function of calcination temperature for 6 wt% Ni/TiO_2 reduced at 500 and 600°C.

interdiffusion between NiO and TiO_2 (9). The observed decrease in the NiO crystallite size as the calcination temperature increase from 300 to 400 or 500°C may be due to the wetting of NiO which resulted from the formation of a $NiTiO_3$ interface between NiO and TiO_2. However, this $NiO/NiTiO_3/TiO_2$ model cannot explain the increased reduction temperature for NiO of ca 10-nm thick site on $NiTiO_3$. The formation of a surface $NiTiO_3$ around the NiO particle may explain both the decreased NiO crystallite and higher reduction temperature. At 600°C, this surface $NiTiO_3$/NiO species further grew into bulk $NiTiO_3$ particles; meanwhile sintering of $NiTiO_3$ might occur as well.

Effect of Reduction Temperature on the Dispersion of Nickel Metal

A decrease in the amount of hydrogen and oxygen adsorbed is accompanied by an increase in the nickel crystallite size with an increasing reduction temperature. The particle sizes of nickel estimated from hydrogen and oxygen chemisorption for selected catalysts are given in Table 2. As it can be seen that comparable values are obtained between XRD and oxygen chemisorption. This is consistent with the result reported by Smith *et al.* that oxygen chemisorption can be used to estimate the nickel particle size for titania-

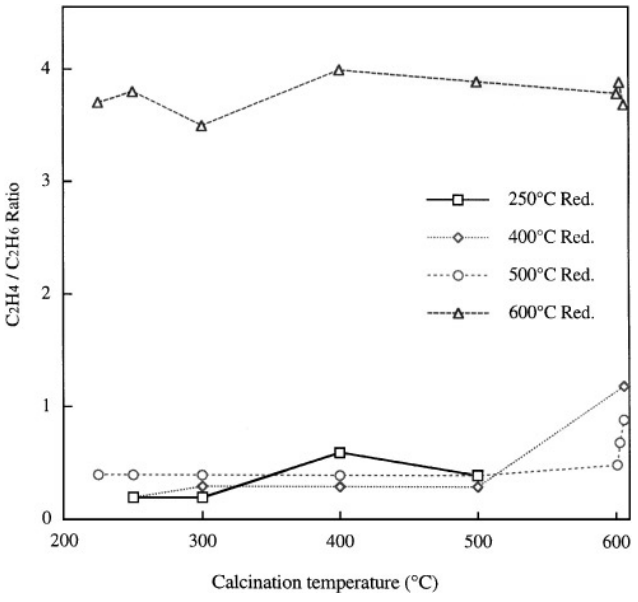

FIG. 11. Variation of ethene to ethane ratio as a function of calcination temperature for 6 wt% Ni/TiO_2 catalysts reduced at various temperatures.

supported nickel (11, 12). The significantly larger particle sizes are obtained from hydrogen chemisorption, indicating a suppression of hydrogen adsorption which was well documented for titania-supported metal (3). The fraction of Ni surface capable of hydrogen adsorption can be represented by H/O adsorption ratio. The H/O ratio as a function of calcination temperature for catalysts reduced at various temperature is shown in Fig. 12. When reduction temperature is from 250 to 500°C, the H/O ratio is not dependent on the reduction or calcination temperature and averages 0.18 ± 0.02. This value is comparable to the reported values (0.26–0.31) for 1.4–12.3% Ni/TiO_2 catalysts reduced at 500°C (20). This means that the adsorption properties of nickel metal are independent on the precursor. The suppression of hydrogen chemisorption on titania-supported metal catalysts is generally accepted to be due to the covering of metal surface by partially reduced TiO_x ($x < 2$) moieties through migration (24, 25), and the extent of suppression is found to increase with increasing the reduction temperature (26). It is unexpected that the extent of hydrogen suppression for all catalysts depends little on the reduction temperature ranged from 250 to 500°C. The migration mechanism is unlikely applicable to catalysts reduced under 300°C. One possible explanation is the source of covering for low temperature reduction may be related the presence of surface $NiTiO_3$ on NiO, as indicated by TPR. After reduction, the segregated TiO_x from surface $NiTiO_3$ remained on nickel metal surface causing the suppression of hydrogen adsorption. Significantly lower H/O ratios that average 0.05 ± 0.01, which is independent on the kind of nickel precursor, are obtained for catalysts reduced at 600°C. A similar behavior was reported by Hoang-Van *et al.* (11); H/O ratios of 0.5 and 0.67 were obtained for 11.3 wt% Ni/TiO_2 catalyst reduced at 300 and 500°C, respectively, but the H/O ratio decreased to zero as the reduction temperature increased to 700°C. This behavior suggests that additional source of suppression of hydrogen adsorption other than the covering by TiO_x moieties exists for titania-supported nickel catalysts reduced ≥600°C.

Effect of Unreduced Nickel Phase on the Activity of Nickel Metal

The variation of TOF(H_2) as a function of the percentage of nickel reduction for some selected catalysts is show in Fig. 13. It is noted that a decrease in TOF(H_2) with a decreasing percentage of nickel reduction was observed for catalysts with higher calcination temperatures (≥400°C), while no significant effect of percentage of nickel reduction was observed for catalysts calcined under 300°C. This may be rationalized by the intimate contact between the unreduced nickel phase and nickel metal which is necessary for the effect of an unreduced nickel phase to occur. Based on the results of XRD, XPS, and TPR, a strong interaction between NiO and TiO_2 occurred when catalysts were calcined above 300°C. Therefore, a better contact between the unreduced nickel phase (possibly surface $NiTiO_3$ or $NiTiO_3$) and nickel metal is expected. The detrimental effect of unreduced metal phase on the activity of metal for CO hydrogenation has been reported for cobalt (27–29). However, the nature of this phenomenon is not clear. The decrease in activity is not accompanied by a change in selectivity, and these TOF(H_2) are still higher than that

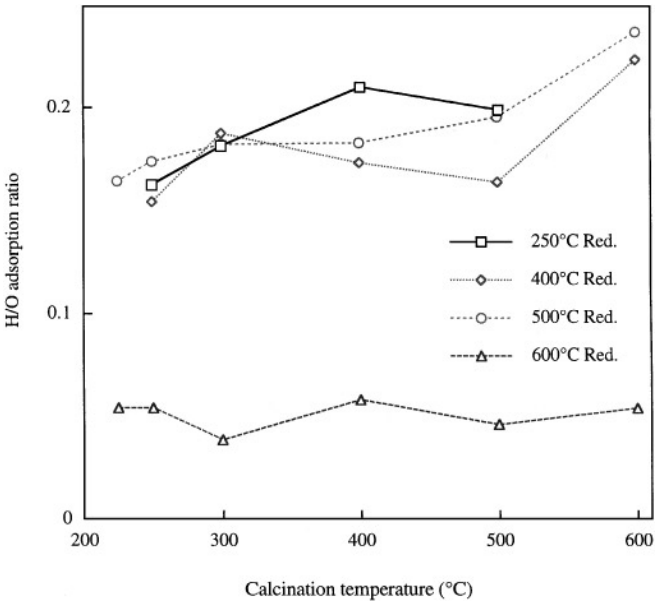

FIG. 12. Variation of H/O adsorption ratio as a function of calcination temperature for 6 wt% Ni/TiO_2 catalysts reduced at various temperatures.

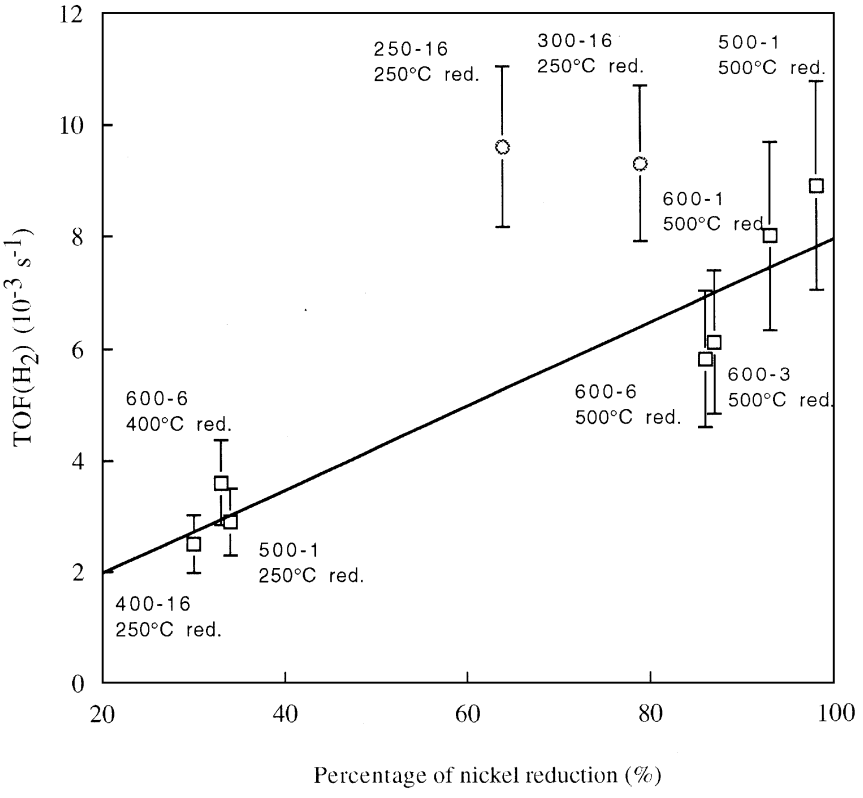

FIG. 13. Turnover frequency, TOF(H_2), versus percentage of nickel reduction.

(5×10^{-4} to 1×10^{-3} s^{-1}, values extrapolated to 200°C) reported for unsupported nickel (30), or silica- (31–33) or alumina-supported nickel (34). Therefore, it is likely that the unreduced nickel phase may hinder the promotion effect of titania, hence, the decrease in activity.

Effect of Reduction Temperature on the Activity of Nickel Metal

In comparison with silica- or alumna-supported nickel catalysts, titania-supported nickel catalysts reduced at 450°C were reported to be more active for CO hydrogenation and to favor higher molecular hydrocarbons (paraffinic) formation (1). The higher activity of titania-supported metal catalysts is generally related to the strong metal-support interaction proposed by Tauster *et al.* (3). However, the rate was found to decrease with increasing reduction temperature up to 647°C and selectivity was unchanged for titania-supported nickel catalysts contrary to the observed trend of SMSI with increasing reduction temperature (5). Nonetheless, an increase in the CO hydrogenation rate was reported for the titania-added nickel–alumina catalysts reduced at 600°C (35), but methane was the dominate product and no higher hydrocarbons were found. In the present study, the activities (μmol/g-Ni/s) of CO hydrogenation and methanation are also found to decrease with increasing the reduction temperature for all Ni/TiO_2 catalysts, despite the fact that each catalyst has various amounts of Ni precursors as NiO, surface $NiTiO_3$, or $NiTiO_3$. This shows the detrimental effect of higher reduction temperatures, which is in agreement with former studies (4–5) and that the formation of $NiTiO_3$ is not a prerequisite for the occurrence of SMSI, as suggested by de Bokx *et al.* (9). However, the TOF(H_2) was found to be dependent on neither the calcination temperature nor the reduction temperature and remained more or less invariant. This reveals the physical blocking of the nickel metal surface by TiO*x* moieties. In addition, the TOF(H_2)'s obtained are comparable to those ($9–15 \times 10^{-3}$ s^{-1}, values extrapolated to 200°C) reported for titania-supported nickel catalysts (36, 37) and are an order of magnitude higher than those reported for unsupported nickel and silica- or alumina-supported nickel (30–34). This indicates the presence of the promotion effect of titania on CO hydrogenation after high-temperature reduction. Despite the decrease in the overall rate per gram of nickel, an increase in the rate of ethene per gram of nickel was observed for all catalysts when the reduction temperature is increased to 600°C as shown in Fig. 14. The change in catalytic property for Ni/TiO_2 catalysts as the reduction temperature increases from 500 to 600°C is further evidenced by an increase in the methane selectivity, the ethene fraction, the C2 to C4 fraction, and the olefin to paraffin ratio of the C2-C4 fraction. The increased methanation rate may be attributed to the more competitive

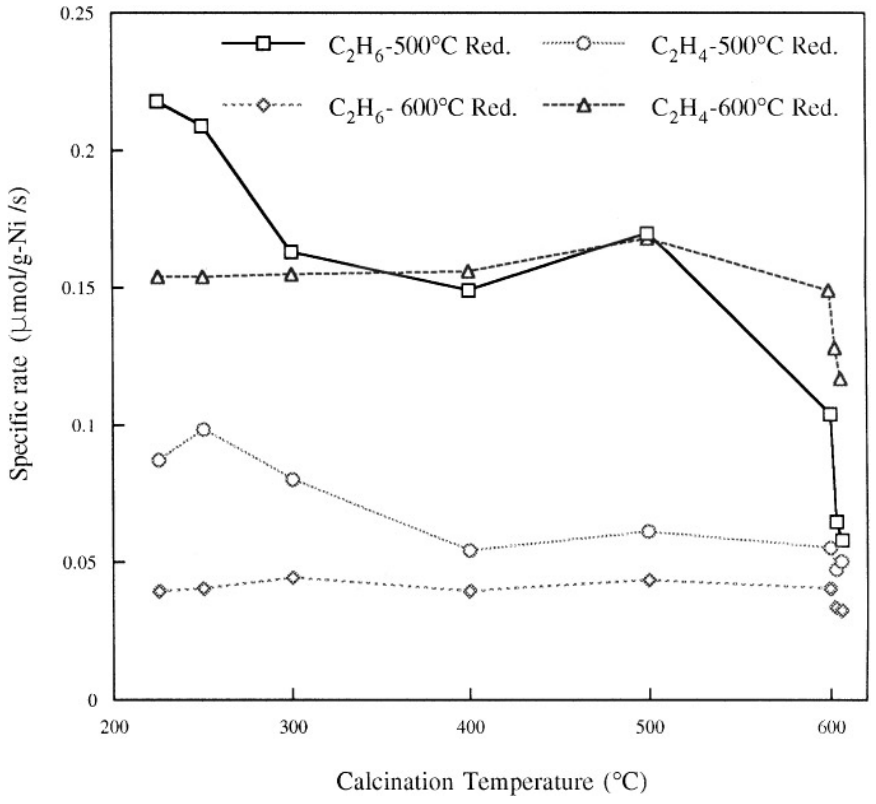

FIG. 14. Variation of rates of ethene and ethane formation as a function of calcination temperature for 6 wt% Ni/TiO_2 catalysts reduced at 500 and 600°C.

hydrogen chemisorption (38) or the increase in the H-adatom concentration (39). The increased ethene formation rate and olefin fraction observed in the present study may also be related to the more competitive hydrogen adsorption on nickel under the influence of TiO_x which forbids the readsorption of olefins for secondary hydrogenation. The dramatic decrease in C5+ fraction indicates a decrease in the chain growth, possibly due to the limited number of carbon species for chain growth on a small area of active nickel surface confined by the covered TiO_x moieties. The modification in catalytic properties accompanies the additional decrease in the fraction of nickel metal capable of hydrogen adsorption. This may be related to the short-ranged electronic effect of the heavily decorated TiO_x with $x \approx 1$ (40, 41).

CONCLUSIONS

The population of nickel species in 6 wt% Ni/TiO_2 catalysts was found to depend on the calcination temperature. For catalysts calcined under 300°C, discrete NiO is the main species. The main nickel species became NiO covered with the surface $NiTiO_3$ compound as the calcination temperature was increased to 400 or 500°C, and finally, discrete $NiTiO_3$ at 600°C. In turn, a dependence of reducibility on the nickel species was observed. For catalysts calcined below 600°C, where NiO is the main nickel species, 100% reducibility can be obtained at a reduction temperature of 400°C. However, for catalysts calcined at 600°C, where $NiTiO_3$ is the dominant nickel species, complete reduction of the nickel species can be achieved at 600°C.

The particle size of Ni estimated from X-ray diffraction and oxygen chemisorption agree, more or less, with each other, while that from hydrogen chemisorption were too large. This is attributed to the suppression of hydrogen chemisorption by the covering of TiO_x moieties on the nickel metal surface. The fraction of nickel surface capable of hydrogen adsorption was estimated from the H/O adsorption ratio. The H/O ratio remains unchanged for all catalysts below 500°C (0.18 ± 0.02), but decreases to one-third for catalysts reduced at 600°C (0.05 ± 0.01), indicating further covering of the nickel surface by TiO_x moieties.

Lower turnover frequencies ($TOF(H_2)$) for CO hydrogenation were obtained for the catalysts with unreduced nickel phase. When nickel is completely reduced, TOF is not dependent of the chemical states of nickel in the calcined catalysts. The invariant $TOF(H_2)$ for catalysts indicates that the decrease in the activity based on per-gram Ni with increasing reduction temperature is due to the increase in the extent of physical blocking of nickel metal surface by TiO_x moieties. Furthermore, the $TOF(H_2)$'s are an order of magnitude higher than that reported for unsupported

nickel, or silica- or alumina-supported nickel catalyst, indicating the promotion effect of titania on CO hydrogenation even after high reduction temperature. However, the selectivity was modified when the reduction temperature was raised to 600°C: (1) enhanced rate for ethene formation (from 0.07 ± 0.02 to 0.15 ± 0.02 μmol/g Ni/s), (2) enhanced methane (from 15 to 28%), C2-C4 (from 30 to 62%), and olefins (C2-C4, from 21 to 56%) formation at the compensation of C5+ fraction (from 55 to 10%). These variations inversely correlate with the extent of hydrogen suppression, suggesting the additional interaction of the decorated TiO_x moieties with nickel surface after reduction at 600°C.

ACKNOWLEDGMENT

This work was supported by the National Science Council, Republic of China.

REFERENCES

1. Vannice, M. A., and Garten, R. L., *J. Catal.* **56**, 236 (1979).
2. Bartholomew, C. H., Pannell, R. B., and Butler, J. L., *J. Catal.* **65**, 335 (1980).
3. Tauster, S. J., Fung, S. C., and Garten, R. L., *J. Am. Chem. Soc.* **100**, 170 (1978).
4. Burch, R., and Flambard, A. R., *J. Catal.* **78**, 389 (1982).
5. Turlier, P., Dalmon, J. A., and Martin, G. A., *Stud. Surf. Sci. Catal.* **11**, 203 (1982).
6. van de Loosdrecht, J., van der Kraan, A. M., van Dillen, A. J., and Geus, J. W., *J. Catal.* **170**, 217 (1997).
7. zur Loye, H.-C., Faltens, T. A., and Stacy, A. M., *J. Am. Chem. Soc.* **108**, 8104 (1988).
8. Asakura, K., Iwasawas, Y., and Kuroda, H., *J. Chem. Soc., Faraday Trans. 1* **84**, 1329 (1988).
9. de Bokx, P. K., Bonne, R. L. C., and Geus, J. W., *Appl. Catal.* **30**, 33 (1987).
10. Klug, H. P., and Alexander, L. E., "X-ray Diffraction Procedures," p. 491. Wiley, New York, 1954.
11. Hoang-Van, C., Kachaya, Y., Teichner, S. J., and Dalmon, J. A., *Appl. Catal.* **46**, 281 (1989).
12. Smith, J. S., Thrower, P. A., and Vannice, M. A., *J. Catal.* **68**, 270 (1981).
13. Kim, K. S., and Davis, R. E., *J. Electron Spectrosc. Relat. Phenom.* **1**, 25 (1972/73).
14. Tomellini, M., *J. Chem. Soc., Faraday Trans. 1* **84**, 3501 (1988).
15. Gonzalez-Elipe, A. R., Holgado, J. P., Alvarez, R., and Munuera, G., *J. Phys. Chem.* **96**, 3080 (1992).
16. Espinos, J. P., Gonzalez-Elipe, A. R., Caballero, A., Garcia, J., and Munuera, G., *J. Catal.* **136**, 415 (1992).
17. Zhang, L., Lin, J., and Chen, Y., *J. Chem. Soc. Faraday Trans. 1* **88**, 2075 (1992).
18. Richardson, J. T., Turk, B., Lei, M., and Forster, K., *Appl. Catal.* **83**, 87 (1992).
19. Solcova, O., Uhristiane, D.-C., Steinike, U., and Jiratova, K., *Appl. Catal.* **94**, 153 (1993).
20. Kumbhar, P. S., *Appl. Catal.* **96**, 241 (1993).
21. Rao, C. N. R., Sankar, G., and Rayment, T., *J. Mater. Chem.* **1**, 299 (1991).
22. Rao, C. N. R., Kulkarni, G. U., Sankar, G., Ranga Rao, G., and Kannan, K. R., *in* "Advances in Catalysts Design" (M. Graziani and C. N. R. Rao, Eds.), p. 1. World Scientific, Singapore, 1991.
23. Beck, D. D., and White, J. M., *J. Phys. Chem.* **88**, 2764 (1984).
24. Simoens, A. J., Baker, R. T. K., Dwyer, D. J., Lund, C. R. F., and Madon, R. J., *J. Catal.* **86**, 359 (1984).
25. Haller, G. L., and Resasco, D. E., *Adv. Catal.* **36**, 173 (1989).
26. Ho, S.-W., Cruz, J. M., Houalla, M., and Hercules, D. M., *J. Catal.* **135**, 173 (1992).
27. Reuel, R. C., and Bartholomew, C. J., *J. Catal.* **85**, 78 (1984).
28. Moon, S. H., and Yoon, K. E., *Appl. Catal.* **16**, 2869 (1985).
29. Turlier, P., Praliaud, H., Moral, P., Martin, G. A., and Dalmon, J. A., *Appl. Catal.* **19**, 287 (1985).
30. Kelly, R. D., and Goodman, D. W., *Surf. Sci.* **123**, L743 (1982).
31. Coulter, K., Xu, X., and Goodman, D. W., *J. Phys. Chem.* **98**, 1245 (1994).
32. Lee, C., Schmidt, L. D., Moulder, J. F., and Rusch, T. W., *J. Catal.* **99**, 472 (1986).
33. Bartholomew, C. H., Pannel, R. B., and Bulter, J. L., *J. Catal.* **65**, 335 (1980).
34. Vannice, M. A., *J. Catal.* **44**, 152 (1976).
35. Lansink Rotgerink, H. G. J., Mercera, P. D. L., Van Ommen, J. G., and Ross, J. R. H., *Appl. Catal.* **45**, 239 (1988).
36. Vannice, M. A., and Garten, R. L., *J. Catal.* **66**, 242 (1980).
37. Vannive, M. A., *J. Catal.* **174**, 199 (1982).
38. Vannice, M. A., Twu, C. C., and Moon, S. H., *J. Catal.* **79**, 70 (1983).
39. Raupp, G. B., and Dumesic, J. A., *J. Catal.* **96**, 597 (1985).
40. Raupp, G. B., and Dumesic, J. A., *J. Catal.* **97**, 85 (1986).
41. Raupp, G. B., and Dumesic, J. A., *J. Catal.* **95**, 587 (1985).